Available online at www.sciencedirect.com
SCIENCE DIRECT®
Journal of Magnetic Resonance 167 (2004) 266–272
JMR Journal of Magnetic Resonance
www.elsevier.com/locate/jmr

Spin-state-selective excitation in gradient-selected heteronuclear cross-polarization NMR experiments

Teodor Parella*

Servei de Ressonància Magnètica Nuclear, Universitat Autònoma de Barcelona, E-08193, Bellaterra, Barcelona, Spain

Received 8 July 2003; revised 5 December 2003

Abstract

Several heteronuclear coherence transfer mechanisms involved in proton-detected heteronuclear *J*-cross-polarization (HCP) NMR experiments have been theoretically derived and experimentally verified in isotropic solution. It is shown that in-phase and/or anti-phase heteronuclear coherence transfer can take place separately or simultaneously during the HCP process as a function of the relative phase between the HCP mixing sequence and the corresponding input magnetization. As the more important consequence, clean coherence-order and spin-state selective (S^3) excitation with maximum sensitivity can be achieved from gradient-enhanced HCP experiments by proper co-addition/subtraction of in-phase and anti-phase magnetizations, offering an attractive alternative to widely used HSQC-type experiments.

Keywords: Spin-state selective excitation; Heteronuclear cross-polarization; Selective inverse experiments

1. Introduction

The HSQC and HMQC pulse schemes are nowadays the most widely accepted NMR pulse trains for heteronuclear coherence transfer in isotropic solution between a high-sensitive I nucleus (typically ^{1}H) and a low-sensitive S nucleus (for instance, ^{13}C or ^{15}N). These NMR techniques rely in the free-evolution of the heteronuclear coupling constant during predetermined J evolution delays combined by magnetization transfer from/to anti-phase or multiple-quantum spin-states via 90° radio-frequency (RF) pulses. However, it is also possible to perform such transference processes using a third approach, the so-called heteronuclear *J*-cross-polarization (HCP) [1–6], sometimes also referred as Heteronuclear Hartmann-Hahn (HEHAHA) or hetero-TOCSY experiments. In the basic HCP experiments, two continuous-wave (CW) RF fields are simultaneously applied to both I and S spins (with intensities $\omega_{1I} = \gamma^I B_1^I/2\pi$ and $\omega_{1S} = \gamma^S B_1^S/2\pi$, respectively) and the transfer becomes efficient when the so-called Hartmann-Hahn condition is fulfilled

$$|\omega_{1I} - \omega_{1S}| \ll J_{IS}. \quad (1)$$

Recently, it has been demonstrated that the use of weak CW RF fields makes HCP an ideal tool for selective experiments in solution state [7–10]. However, they lead to a strong offset dependence of the Hartmann-Hahn condition and a match can be only achieved for small frequency ranges. In more demanding non-selective applications, broadband HCP must be accomplished using optimized multiple-pulse sequences [6].

In theory, the transfer efficiency for all three HMQC, HSQC, and HCP processes are the same but, in practice, the usage of the HCP transfer mechanism has been limited in a few cases. Among others, specific NMR pulse sequences making use of ^{1}H–X HCP [11,12] have been described for small molecules at natural abundance (X = ^{13}C) [13–16], for large and isotopically labelled biomolecules (X = ^{13}C and ^{15}N) [17–20], and also successfully applied to other heteronuclei such as ^{31}P [21,22] or ^{113}Cd [23,24].

However, HCP mixing process offers a unique feature that, in my knowledge, has been never exploited.

* Fax: +34-93-5812291.
E-mail address: teo@rmn3.uab.es.

1090-7807/$ - see front matter © 2004 Elsevier Inc. All rights reserved.
doi:10.1016/j.jmr.2004.01.002

Generation of in-phase and anti-phase coherence transfer during the HCP process can occur separately or simultaneously and, therefore, it should be possible to combine them to afford spin-state-selective (S^3) states which are defined as the sum or difference of such in-phase and anti-phase magnetizations:

$$I^- S^{\alpha} = I^- + 2I^- S_z, \tag{2a}$$

$$I^- S^{\beta} = I^- - 2I^- S_z. \tag{2b}$$

Two different approaches have been employed to generate these particular S^3 states. In-phase and anti-phase magnetizations can be recorded in separate spectra and then they are added/subtracted to yield the two mentioned α and β sub-spectra. On the other hand, it is also possible to generate the S^3 states directly in a single experiment by selecting both coherences just prior to acquisition.

For the first time, in this work we show that the S^3 principle [25–27] can be incorporated in HCP-based pulse schemes by using coherence-order selection by pulsed-field gradients. In particular, we demonstrate this feature using a gradient-enhanced 1D spin-state-selective HCP (α, β-HCP) experiment in order to obtain clean S^3 excitation from high-quality artefact-free spectra displaying maximum sensitivity, similarly as reported previously for the spin-edited HMQC and HSQC experiments [28,29]. The main feature of the proposed 1D α, β-HCP experiment is that the α or β state of the heteronucleus is selected by simple inversion of the phase of a non-selective 90° X pulse just after the HCP process or, alternatively, by changing the gradient ratio used for coherence selection. Closely related to the principles outlined here, spin-state selection using single-transition HCP has been also proposed by applying selective CW spin-lock fields to a pair of connected transitions [30–33].

2. Results and discussion

The possibility to obtain separately in-phase or anti-phase proton magnetization (with respect to the ^1J(CH) coupling constant) from 1D carbon-selective HCP experiments was already pointed out simply by proper choice of some 90° proton and carbon pulses embedding the HCP block [16]. Based on this idea, attention has been focused on the study of the different coherence transfer mechanisms involved during the HCP mixing processes. For simplicity, we have designed the 1D pulse scheme displayed in Fig. 1 in which offset effects have been avoided by setting the carrier frequency on-resonance of the selected signals. The sequence has been adapted from the two-way doubly selective cross-polarization experiment [8,9] and it can be understood as the 1D gradient-enhanced version of the original 2D

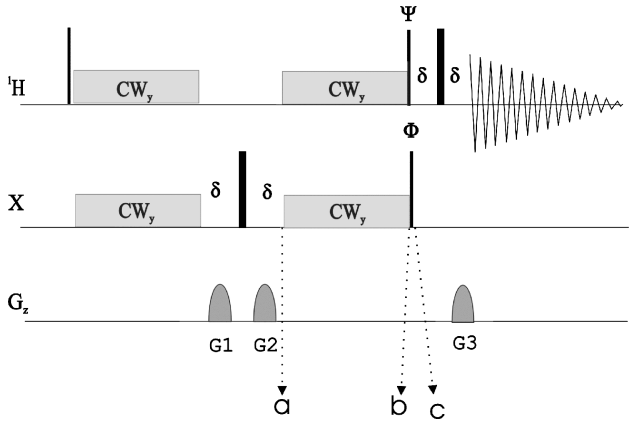

Fig. 1. Pulse sequence diagram of the gradient-selected 1D selective heteronuclear cross-polarization (HCP) experiment. A four-step EXORXYCLE phase cycle is applied on the central X 180° pulse $(x, y, -x, -y)$ and the receiver $(x, -x)$. The CW spin-lock fields are simultaneously applied in both channels, from the y axis and with a duration Δ, in both preparation and mixing HCP periods. Gradients of duration (δ) of 1 ms, with a recovery time of 100 μs are also indicated by shaded shapes on the line G_z. Frequency carriers are set on resonance of the selected signals through all experiment. See text and Table 1 for details about the Φ and Ψ phases of the last 90° pulses and about the gradient ratios.

HCP experiment described some years ago [6]. After the initial 90°(I) pulse applied from the x axis, selective coherence transfer takes place during the doubly selective HCP(y) period, optimized to $\tau_m = 1/^1J(IS)$, where cross-polarization and selective excitation is performed simultaneously by applying very weak RF continuous-wave fields from the y axis. It has been demonstrated that under these conditions, the Hartmann-Hahn condition need not be fulfilled accurately and inhomogeneous RF fields do not significantly affect the transfer efficiency [7]. The resulting in-phase S magnetization is allowed to evolve during a gradient-encoding spin-echo period in which heteronuclear coupling constants and S chemical shift are fully refocused by the effect of the 180° S pulse. After this de-phasing period, a second HCP(y) block identical to the first block, transfers back the selected transverse S magnetization to the directly attached I nucleus via the active $^1J(IS)$ coupling constant, whose magnetization is finally refocused with the last G_3 gradient echo and detected with optional heteronuclear decoupling.

In the case of $I = {}^1$H and $S = {}^{13}$C, the general equation for proper gradient refocusing in the α, β-HCP experiment can be written as

$$p_1 G_1 + p_2 G_2 - 4G_3 = 0, \tag{3}$$

where p_i defines the selected coherence order during the G_i gradient. The same pulse sequence can be executed with and without gradient coherence selection. Using a 1:1:0 gradient ratio, a phase-cycled 1D HCP spectrum is obtained showing full sensitivity but at expense of frequently poor spectral quality due to imperfect ^{1}H–^{12}C

suppression when applied on natural abundance samples. On the other hand, gradient coherence selection using for instance a −2:2:1 gradient ratio affords ultra-clean 1D spectra but, in principle, with theoretical sensitivity losses due to specific coherence selection during the transverse S evolution period.

The sequence of Fig. 1 is suitable to study the presence and the efficiency of several heteronuclear transfer mechanisms from S to I nucleus via the last HCP mixing process. These mechanisms greatly depend on the relative phase between the input S magnetization available just prior to the HCP process and the HCP RF fields. Detailed description on the theory of coherence polarization transfer using selective cross-polarization in solution state have been extensively described [7–9] and, therefore, minor details will be given here. In absence of offset dependences and unwanted mismatch of the Hartmann-Hahn condition, the effective coupling term of the active Hamiltonian during the HCP process applied from the y axis can be reduced to

$$H^{\text{eff}} = \pi J_{IS}^{\text{eff}}(2I_zS_z + 2I_xS_x). \tag{4}$$

In heteronuclear experiments, the effective coupling constant is usually given by $J_{IS}^{\text{eff}} = J_{IS}/2$ [34]. Under these conditions, the theoretical efficiency transfer for the so-called parallel S_y component in a IS spin system is defined as follows:

$$S_y \xrightarrow{\text{HCP}_y} \frac{1+\cos(\pi J_{IS}\tau)}{2}S_y + \frac{1-\cos(\pi J_{IS}\tau)}{2}I_y + (2I_xS_z - 2I_zS_x)\frac{\sin(\pi J_{IS}\tau)}{2}. \tag{5a}$$

The HCP concept has been commonly used to achieve efficient in-phase to in-phase heteronuclear transfer when the HCP mixing time is adjusted to $\tau = 1/J_{IS}$ for IS spin systems. However, a different behaviour arises when the input S coherence is perpendicular to the HCP process:

$$S_x \xrightarrow{\text{HCP}_y} S_x\cos\left(\frac{\pi J_{IS}\tau}{2}\right) + 2S_yI_z\sin\left(\frac{\pi J_{IS}\tau}{2}\right), \tag{5b}$$

$$S_z \xrightarrow{\text{HCP}_y} S_z\cos\left(\frac{\pi J_{IS}\tau}{2}\right) + 2S_yI_x\sin\left(\frac{\pi J_{IS}\tau}{2}\right). \tag{5c}$$

In such cases, after the optimum $\tau = 1/J_{IS}$ mixing period, both S_x or S_z magnetizations are fully converted to anti-phase S_yI_z and multiple-quantum S_yI_x magnetizations, respectively.

The three different mechanisms described by Eqs. (5a)–(5c) were experimentally and independently verified using simple modifications of the proposed HCP experiment of Fig. 1 in which the gradient ratio was adjusted to 1:1:0 (the last echo period prior to acquisition is not applied), the amplitudes of the CW RF fields were matched to $\gamma^I B_1^I/2\pi = \gamma^S B_1^S/2\pi = 75$ Hz and placed on resonance to the selected ^{1}H and ^{12}C resonances of a sample of strychnine. According to Eq. (5a), the normal full-sensitivity in-phase doublet is achieved under conventional HCP(y) transfer (Fig. 2B) in which the last simultaneous 90° (I,S) pulses are omitted.

$$S_y \xrightarrow{HCP_y(\tau=1/J)} I_y. \tag{6a}$$

The signal-to-noise (S/N) ratio of this 1D spectrum is taken as the reference to check the overall sensitivity for all other transfer mechanisms discussed below. On the other hand, the perpendicular $S_x \xrightarrow{\text{HCP}_y} S_yI_z$ transfer (see Eq. 5b) is demonstrated by shifting the initial 90°$_x$(I)-HCP(y) block to a 90°$_y$(I)-HCP(x) block that generates the desired input S_x coherence. The resulting anti-phase S_yI_z magnetization after the second HCP scheme is converted to observable anti-phase S_zI_y magnetization by applying two simultaneous 90°(I,S) pulses from the x axis (Fig. 2C)

$$S_x \xrightarrow{\text{HCP}_y(\tau=1/J)} 2S_yI_z \xrightarrow[90°_x(S)]{90°_x(I)} -2S_zI_y. \tag{6b}$$

Finally, the perpendicular $S_z \xrightarrow{\text{HCP}_y} S_yI_x$ transfer (Fig. 2D) is also confirmed by converting the initial S_y magnetization to S_z by a 90°$_x$(S) pulse prior to the second HCP(y) process and converting the final anti-phase S_yI_z magnetization (see Eq. 5c) to observable magnetization by a single 90°(S) pulse applied from the x axis:

$$S_y \xrightarrow{90°_x(S)} S_z \xrightarrow{\text{HCP}_y(\tau=1/J)} 2S_yI_x \xrightarrow{90°_x(S)} 2S_zI_x. \tag{6c}$$

From all these 1D HCP spectra, it can be stated that effective in-phase and anti-phase coherence transfer can be achieved with maximum sensitivity but spectral quality can suffer of the inefficient phase cycling procedure.

A different behaviour occurs when using gradient coherence selection in the 1D HCP experiment. Assuming that a −2:2:1 gradient ratio selects the $p_1 = -1$ and $p_2 = +1$ coherence orders, the available transverse S magnetization after the first HCP(y) block is better described using shift-operators and, therefore, such available coherences must be treated as a mixture of transverse S_x and S_y components. As described above, the effect of the second HCP(y) process for each one of these orthogonal in-phase magnetizations (Eqs. (5a)–(5c)) will depend of their relative phases.

$$S^- = S_x - \mathrm{i}S_y \xrightarrow{180°_x(S)} S^+ = S_x + \mathrm{i}S_y \xrightarrow{HCP_y} 2S_yI_z + \mathrm{i}I_y. \tag{7}$$

The crucial point of the strategy proposed here relies on the setting and the effect of the phases of the 90°(I) pulse (with phase Ψ) and the 90°(S) pulse (with phase Φ) applied just after the second HCP process and before the refocusing gradient echo (Table 1). When $\Psi = \Phi = y$, the conventional in-phase doublet is obtained with perfect suppression of ^{1}H–^{12}C magnetization (Fig. 3A) but a decrease of the overall sensitivity by a factor of two results when compared to the analogous phase cycle

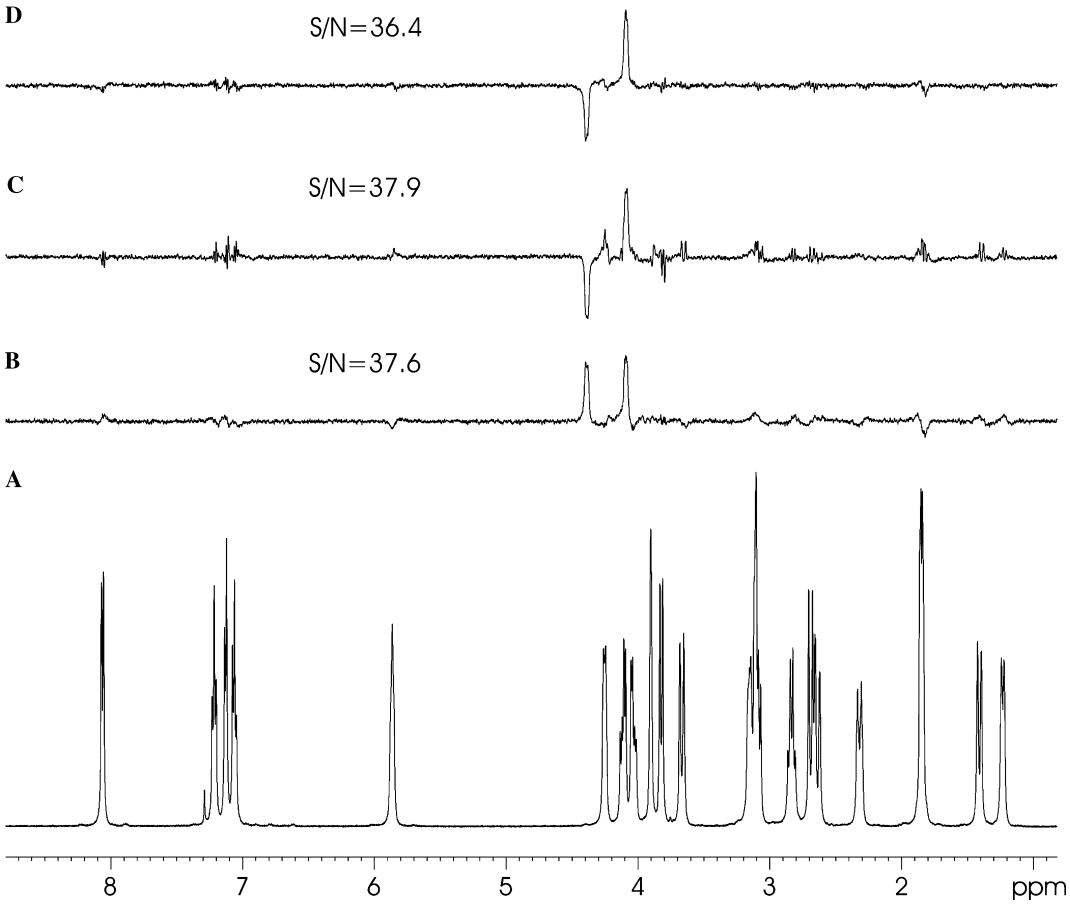

Fig. 2. (A) Conventional ^{1}H 500 MHz spectrum of strychnine in $CDCl_3$; (B–D) Several phase-cycled 1D HCP spectra acquired with the sequence of Fig. 1 with a 1:1:0 gradient ratio: (B) $S_y \xrightarrow{HCP_y} I_y$ (Eq. 5a), (C) $S_x \xrightarrow{HCP_y} S_y I_z$ (Eq. 5b), and (D) $S_z \xrightarrow{HCP_y} S_y I_x$ (Eq. 5c) HCP transfers after selective cross-polarization of the H_{12}–C_{12} pair. In (B) the 90° pulses (labelled with phases Φ and Ψ) are not applied (see Eq. 6a). In (C) both 90° ^{1}H and ^{13}C pulses (applied from x axis) are applied just after the HCP mixing scheme to observe the corresponding proton signal, as described in Eq. 6b. In (D) only the 90° ^{13}C pulse (applied from the x axis) is applied after the HCP process to observe the anti-phase proton signal as described in Eq. 6c. The experimental signal-to-noise ratios are displayed for each spectrum only for comparison purposes. See text for more details.

Table 1
Product operators available at different points of the HCP pulse sequence as a function of the phases Φ and Ψ (see Fig. 1 for details)

Experiment	Before the HCP (point a)	After the HCP (point b)	Phase of 90° pulses		After the simultaneous 90° (^{1}H,X) pulses (point *c*)
			Ψ	Φ	
1	$S_x + iS_y$	$2I_zS_y + iI_y$	y	y	$-2I_xS_y + iI_y$
2			x	x	$2I_yS_z + iI_z$
3			y	x	$-2I_xS_z + iI_y$
4			y	$-x$	$2I_xS_z + iI_y$
5	$S_x + iS_z$[a]	$2I_zS_y + 2iI_xS_y$	x	x	$-2I_yS_z + 2iI_xS_z$

[a] A $90°_x(S)$ pulse is applied before the HCP(y) process.

experiment, because the second term stands for non-observable multiple-quantum coherences (entry 1 in Table 1).

The anti-phase component (Fig. 3B) can be obtained by applying $\Psi = \Phi = x$, with the corresponding sensitivity penalty (entry 2 in Table 1). However, both in-phase and anti-phase magnetizations can be simultaneously detected (S^3 excitation) by applying $\Phi = y$ and $\Psi = +x/-x$ (Figs. 3C and D, respectively). In this case, the recorded signal shows maximum intensity because of the preservation of equivalent pathways (entries 3–4 in Table 1). The same S^3 editing could be also achieved

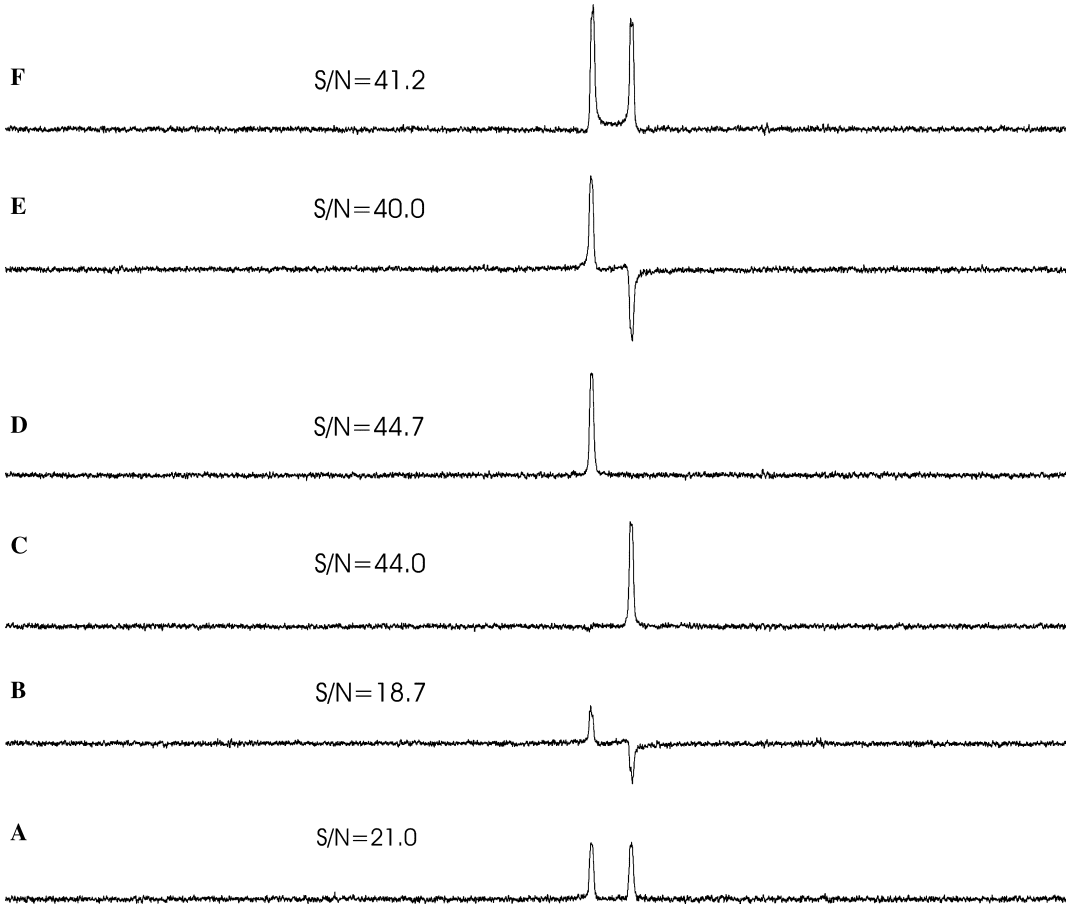

Fig. 3. (A–F) Several 1D gradient-selected HCP spectra acquired with the same conditions as described in Fig. 2 but with coherence selection using a $-2:2:1$ gradient ratio and the following pulse phases: (A) in-phase multiplet obtained with $\Psi = \Phi = y$; (B) anti-phase multiplet obtained with $\Psi = \Phi = x$; (C) α spin-state multiplet obtained with $\Psi = y$ and $\Phi = x$; (D) β spin-state multiplet obtained with $\Psi = y$ and $\Phi = -x$; (E) sensitivity-improved anti-phase multiplet acquired as (B) but with an additional 90°(S) pulse from the x axis before the last HCP mixing process; (F) as (E) but with refocusing of the heteronuclear coupling during the last echo period. The experimental signal-to-noise ratios are displayed for each spectrum only for comparison purposes and they are related to those of Fig. 2. See text and Table 1 for more details.

using equivalent alternatives. For instance, by inverting the strength of the G_3 refocusing gradient instead to invert the Ψ phase or by creating $S_z \pm iS_y$ as input magnetization in the HCP transfer, instead of the described $S_x \pm iS_y$, by means of a $90°_y(S)$–HCP(y)–$90°_{x/-x}(S)$ mixing process.

On the other hand, ultra-clean anti-phase magnetization with maximum sensitivity (Fig. 3E) could be achieved by inserting a 90°(S) pulse from the x axis prior to the HCP(y) process and setting the pulse phases to $\Psi = \Phi = x$ (entry 5 in Table 1). In this case, the detected anti-phase signal is constructed from two different anti-phase components of the same amplitude that can optionally be converted to in-phase signal by including an additional 180°(S) pulse simultaneously to the last 180°(I) in order to allow heteronuclear J coupling evolution. Because the normal duration of this echo is around the same order of the needed evolution delay (about 1.5–1.75 ms), this option has a limited penalty in sensitivity due to extra relaxation losses. The result is a perfect and clean in-phase multiplet (Fig. 3F), showing similar sensitivity ratios of the original phase cycled experiment (Fig. 2B).

Fig. 4 shows different experimental signal intensity dependence vs. the mixing HCP duration (Δ) for all mechanism HCP transfers already described (see caption for details). Good correlation is observed with the theoretical amplitude factors derived from Eqs. (5a)–(5c) and maximum transfer is always achieved at multiples cycles of $1/J$. It can be also seen that the anti-phase doublet in Fig. 4B is clearly inverted at 19 ms ($\Delta = 3/J$) compared to 6 ms ($\Delta = 1/J$) according to the sine dependence described in Eq. 5b. The α, β-HCP experiment also shows high tolerance to mismatch of the mixing HCP delay in a range of 20% of its theoretical value in where undesired spin-state cross-talk are largely minimized (Fig. 4C).

When comparing the proposed α, β-HCP experiment to the previously reported α, β-HMQC and α, β-HSQC experiments [28], we found that α, β-HCP is the more sensitive approach (Fig. 5). The HCP pulse scheme is

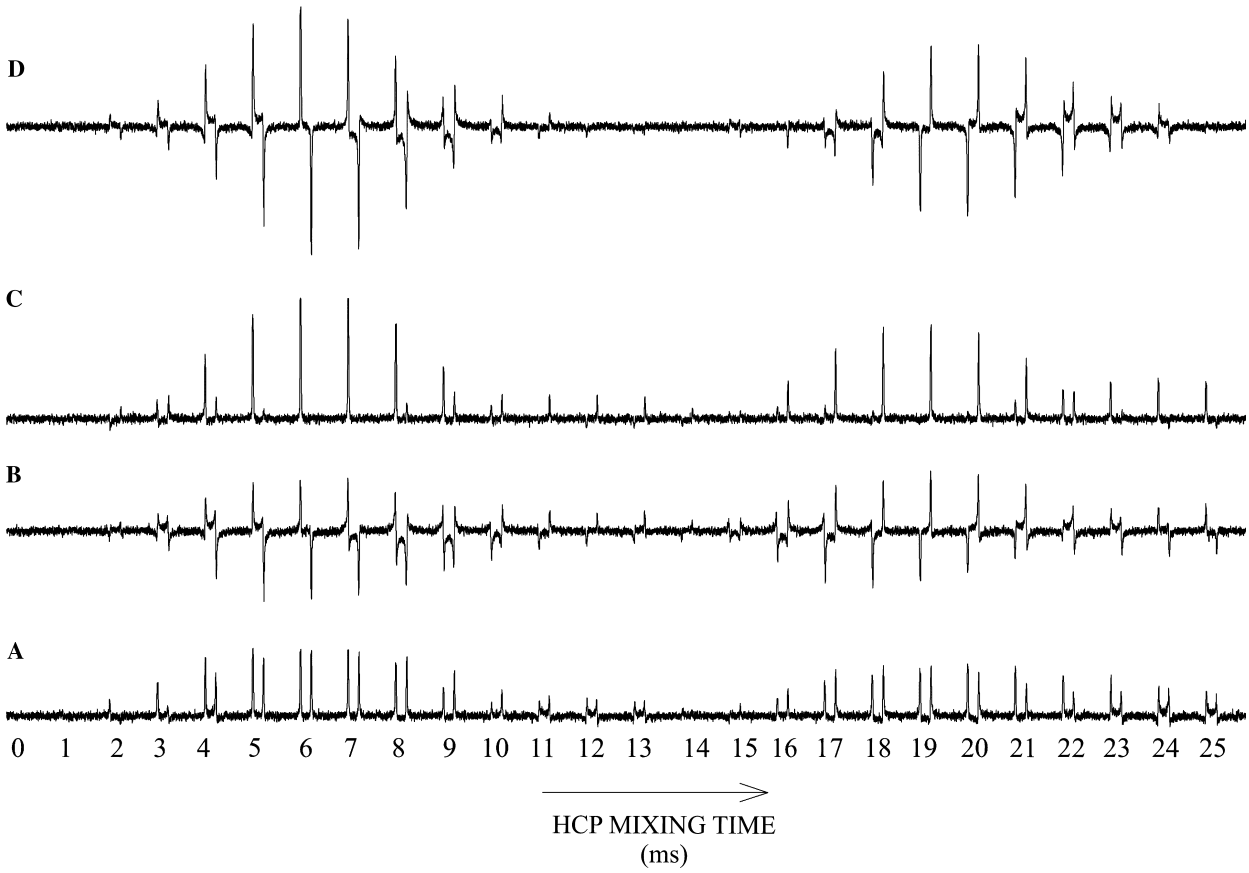

Fig. 4. Experimental signal intensity dependence of the HCP mechanism transfers described in Figs. 3A (A), 3B (B), Fig. 3D (C), and Figs. 3E (D) as a function of the HCP duration (Δ). Twenty-six 1D spectra have been recorded varying the duration of the HCP mixing process from 0 to 25 ms, with an increment value of 1 ms. All other acquisition parameters as described in Fig. 3.

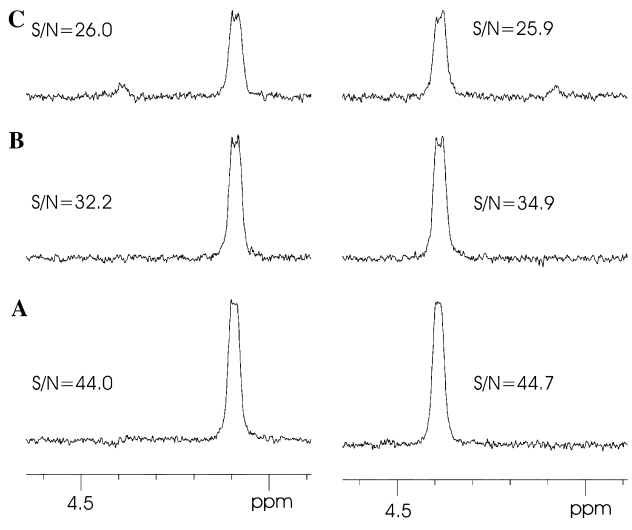

Fig. 5. Comparison of experimental sensitivity ratios of the gradient-selected spin-state-selective (A) α,β-HCP using CW (Fig. 1B), (B) α,β-HMQC experiments [28], and (C) α,β-HSQC experiments [28]. The experimental conditions of (A) are as described in the legend of Fig. 3C. For (B) and (C), a 6 ms 90° Gaussian-shaped pulse was used for selective carbon excitation, and the J evolution delay was optimized to 147 Hz.

more tolerable to miscalibrated pulses and RF inhomogeneities, mixing contact periods can be finely adjusted in time and selectivity and, in addition, the HCP experiment presents better selective-excitation capabilities due to its double-selective nature. It was already noted that selective HCP process was more selective when compared to selective INEPT experiments [7].

3. Conclusions

In summary, it has been demonstrated that is feasible to achieve coherence-order S^3 excitation in heteronuclear cross-polarization experiments as usually performed in related HSQC experiments. The combination of heteronuclear gradient echoes and the preservation of equivalent pathways methodology affords sensitivity-enhanced HCP spectra displaying in-phase, anti-phase or spin-state-selective states without need of extra delays, only considering the phases of the elements defining the mixing HCP process or setting the gradient ratios accordingly. This feature makes of the suggested HCP experiment a highly useful alternative to widely

used free-precession INEPT-based pulse schemes to perform specific spin-state coherence transfers or to measure scalar and dipolar coupling constants. It can be anticipated that the principles described here can be also implemented in higher dimensionality NMR pulse schemes. Much work on the possible applications of the proposed approach is in progress.

4. Experimental part

NMR experiments have been recorded on a BRUKER AVANCE 500 MHz spectrometer at 298 K equipped with a triple-resonance inverse probehead incorporating a z-gradient coil. All ^{1}H and ^{13}C pulses have been applied on-resonance to the selected H12–C12 pair of strychnine ($^1J(\mathrm{CH}) = 147$ Hz) in a sample of 50 mg of product dissolved in $CDCl_3$. The following experimental conditions were applied: relaxation delay of 1 s, HCP mixing delay of $\Delta = 1/J(\mathrm{CH}) = 6.6$ ms and 16 transients with two dummy scans were acquired for all 1D spectra.

The amplitudes of the CW RF fields have been approximately matched to $\gamma^I B_1^I/2\pi = \gamma^S B_1^S/2\pi = {}^1J(\mathrm{CH})/2$ Hz and placed on resonance to the desired signals. Calibration of the power levels and durations for CW irradiation were performed by maximizing the selected signal intensity from the corresponding 1D spectrum.

Acknowledgments

I am indebted to Prof. S.J. Glaser and the referees for their helpful comments and discussions. Financial support for this research provided by MCYT (project BQU2003-01677) is gratefully acknowledged. We thank the Servei de Ressonància Magnètica Nuclear, UAB, for allocating instrument time to this project.

References

[1] L. Muller, R.R. Ernst, Mol. Phys. 38 (1979) 963–967.
[2] D.W. Bertrand, W.B. Moniz, A.N. Garroway, G.C. Chingas, J. Am. Chem. Soc. 100 (1978) 5227–5229.
[3] D.W. Bearden, L.R. Brown, Chem. Phys. Lett. 163 (1989) 432–436.
[4] E.R.P. Zuiderweg, J. Magn. Reson. 89 (1990) 533–542.
[5] M.H. Levitt, J. Chem. Phys. 94 (1991) 30–38.
[6] M. Ernst, C. Griesinger, R.R. Ernst, W. Bermel, Mol. Phys. 74 (1991) 219–252.
[7] E. Chiarparin, P. Pelupessy, G. Bodenhausen, Mol. Phys. 95 (1998) 759–767.
[8] P. Pelupessy, E. Chiarparin, G. Bodenhausen, J. Magn. Reson. 138 (1999) 178–181.
[9] P. Pelupessy, E. Chiarparin, Conc. Magn. Reson. 12 (2000) 103–124.
[10] T.R. Eykyn, D.J. Philp, P.W. Kuchel, J. Chem. Phys. 118 (2003) 6997–7004.
[11] J. Schleucher, M. Schwendinger, M. Sattler, P. Schmidt, O. Schedletzky, S.J. Glaser, O.W. Sorensen, C. Griesinger, J. Biomol. NMR 4 (1994) 301–306.
[12] M. Sattler, P. Schmidt, J. Schleucher, O. Schedletzky, S.J. Glaser, C. Griesinger, J. Magn. Reson. B 108 (1995) 235–242.
[13] J. Shen, J. Magn. Reson. A 119 (1996) 101–104.
[14] C. Dalvit, G. Bovermann, J. Magn. Reson. A 109 (1994) 113–116.
[15] T. Fäcke, S. Berger, J. Am. Chem. Soc. 117 (1995) 9547–9550.
[16] T. Parella, J. Belloc, F. Sánchez-Ferrando, A. Virgili, Magn. Reson. Chem. 37 (1999) 631–636.
[17] J.M. Richardson, R.T. Clowes, W. Boucher, P.J. Domaille, C.H. Hardman, J. Keeler, E.D. Laue, J. Magn. Reson. B 101 (1993) 223–227.
[18] A. Majumdar, E.R.P. Zuiderweg, J. Magn. Reson. A 113 (1995) 19–31.
[19] H. Wang, E.R.P. Zuiderweg, J. Biomol. NMR 5 (1995) 207–211.
[20] E. Chiarparin, P. Pelupessy, B. Cutting, T.R. Eykyn, G. Bodenhausen, J. Biomol. NMR 13 (1999) 61–65.
[21] G.W. Kellogg, J. Magn. Reson. 98 (1992) 176–182.
[22] G.W. Kellogg, A.A. Szewczak, P.B. Moore, J. Am. Chem. Soc. 114 (1992) 2727–2728.
[23] G.W. Kellogg, B.I. Schweitzer, J. Biomol. NMR 3 (1993) 577–595.
[24] B.I. Schweitzer, K.H. Gardner, G. Tucker-Kellogg, J. Biomol. NMR 6 (1995) 180–188.
[25] M.D. Sorensen, A. Meissner, O.W. Sorensen, J. Biomol. NMR 10 (1997) 181–186.
[26] A. Meissner, J.O. Duus, O.W. Sorensen, J. Magn. Reson. 128 (1997) 92–97.
[27] M.D. Sorensen, A. Meissner, O.W. Sorensen, J. Magn. Reson. 137 (1999) 237–242.
[28] T. Parella, J. Belloc, J. Magn. Reson. 148 (2001) 78–87.
[29] A. Ross, M. Czisch, T.A. Holak, J. Magn. Reson. A 118 (1996) 221–226.
[30] T.R. Eykyn, F. Ferrage, G. Bodenhausen, J. Chem. Phys. 116 (2002) 10041–10050.
[31] F. Ferrage, T.R. Eykyn, G. Bodenhausen, J. Chem. Phys. 113 (2000) 1081–1087.
[32] F. Ferrage, T.R. Eykyn, G. Bodenhausen, J. Am. Chem. Soc. 124 (2002) 2076–2077.
[33] T.R. Eykyn, F. Ferrage, E. Winterfors, G. Bodenhausen, ChemPhysChem 4 (2000) 217–221.
[34] S. Glaser, J.J. Quant, in: W.S. Warren, (Ed.), Advances in Magnetic and Optical Resonance, vol. 19, 1996, pp. 59–251.